Journal of Colloid and Interface Science 536 (2019) 507–515

Contents lists available at ScienceDirect

Journal of Colloid and Interface Science

journal homepage: www.elsevier.com/locate/jcis

Regular Article

Lubricant-infused slippery surfaces: Facile fabrication, unique liquid repellence and antireflective properties

Qi Li, Zhiguang Guo *

Hubei Collaborative Innovation Centre for Advanced Organic Chemical Materials and Ministry of Education Key Laboratory for the Green Preparation and Application of Functional Materials, Hubei University, Wuhan, People's Republic of China
State Key Laboratory of Solid Lubrication, Lanzhou Institute of Chemical Physics, Chinese Academy of Sciences, Lanzhou, People's Republic of China

GRAPHICAL ABSTRACT

A lubricant infused slippery and transparent surface was fabricated by introducing a facile spin-coating approach, which exhibited multifunction including promising liquid repellence, anti-icing, self-cleaning properties and mechanical resistance.

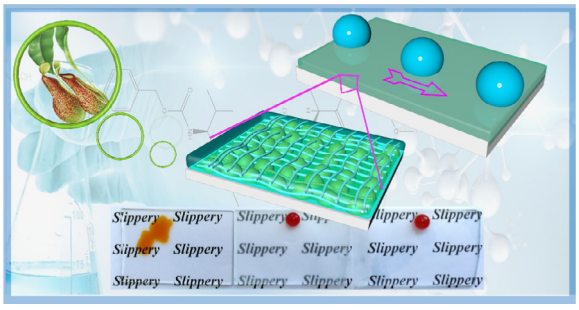

ARTICLE INFO

Article history:
Received 7 September 2018
Revised 25 October 2018
Accepted 25 October 2018
Available online 26 October 2018

Keywords:
Slippery surfaces
Anti-reflective
Omniphobic
Hydrophobic

ABSTRACT

Versatile biomimetic materials possess exceptional functions to address practical challenges in a wide variety of industries. Lubricant-infused slippery (LIS) surfaces that imitate the microstructure of carnivorous nepenthes can repel water and various organic solutions. These materials are manufactured via the infusion of lubricant oil into porous surfaces, a process which yields interfaces that allow other fluids that contact those surfaces to slide off readily. Herein, a facile spin-coating strategy was introduced to construct LIS surfaces. Three kinds of silanes (Tetraethylorthosilicat (TEOS), vinyltriethoxysilane (VTES) and 1H,1H,2H,2H-perfluoroalkyltriethoxysilanes (POTS)) and a UV-curing adhesive were adopted to fabricate an omniphobic coating. After the lubricant (perfluoroalkylpolyether (PFPE)) infusion, the prepared LIS surfaces exhibited an excellent liquid repellent property and positive anti-reflectivity, self-cleaning, anti-icing, anti-corrosion and mechanical resistance properties. The results of this research indicated that this LIS surface can facilitate the manufacture of transparent and multi-functional slippery materials by means of straightforward procedures.

1. Introduction

Endowing surfaces with liquid repellent has aroused much attention since it is critical for infrastructure applications in our daily lives, including applications in liquid transportation [1–4],

* Corresponding author at: Hubei Collaborative Innovation Centre for Advanced Organic Chemical Materials and Ministry of Education Key Laboratory for the Green Preparation and Application of Functional Materials, Hubei University, Wuhan, People's Republic of China.
E-mail address: zguo@licp.cas.cn (Z. Guo).

https://doi.org/10.1016/j.jcis.2018.10.083
0021-9797/

microfluidic devices [5–7], non-fouling marine devices [8,9], and anti-icing [10–12]. Currently, artificial superhydrophobic materials inspired by lotus leaves [13], butterfly wings [14], striders [15], etc., have been extensively explored. The micro-/nano-hierarchical rough structures of superhydrophobic surfaces (SHSs) are modified with low surface energy compounds, which are able to hold air and achieve a Cassie–Baxter state to prevent surfaces from being wetted by water droplets [16–18]. However, most SHSs still have some shortcomings in practical applications. For example, SHSs have poor anti-wetting properties with respect to organic liquids with low surface tension. The hierarchical structure of surfaces can be destroyed by the accumulated ice and frost since micro-droplets easily penetrate textural structures under low temperatures and relatively high humidity surroundings [19–21]. Furthermore, the surface morphologies of most reported superhydrophobic materials are not capable of bearing external mechanical forces [22,23]. Herein, it is meaningful to introduce LIS surfaces to upgrade SHSs for the purpose of eliminating weaknesses.

Carnivorous nepenthes are able to catch insects. The peristome of nepenthes is composed of hydrophilic components and microscopic rough structures that can store water to form a lubricating water film. When insects stay at the peristome, it can easily slide into the digestive system of nepenthes since the water film greatly reduces the friction [24]. This inspires the design of well-known LIS surfaces [25–27]. Compared to SHSs, designing LIS surfaces only requires low surface roughness. Recently, this type of biologically inspired surface design has become an emerging class for preparing multi-functional materials that exert unique liquid-repellent abilities toward nearly all types of liquids. Surfaces presenting excellent slippery characteristics have the potential to be used in robust anti-icing, anti-fouling [10,28], and slippery containers for the preservation and distribution of commercial liquids and gels [29].

At present, there are mainly two different methods for preparing LIS surfaces. The first pathway is related to the construction of micro-/nano-hierarchical porous structures modified with low surface energy. Based on this approach, abundant studies on manufacturing slippery surfaces have been reported. Wong et al. achieved surfaces where liquids slid freely by designing hierarchical micropillars on matrixes with the aid of soft polymeric materials [30]. Wang et al. reported a brushing technique for designing LIS surfaces that mainly involved infusing lubricant into porous composed of nanoparticle–polymer gel [31]. The previous studies of Sun and coworkers reported on LIS surfaces with a porous microstructure that were formed by virtue of a hydrothermal method [32]. Another route to form LIS surfaces is associated with the introduction of cross-linked polymer networks or a free volume structure [33,34], which can lock or encapsulate the infused lubricant in the substrate surface for a long time. Ragogna et al. utilized UV cross-linked, interpenetrated siloxane polymer networks to improve the durability of LIS surfaces [35]. Shiratori et al fabricated temperature-activated solidifiable/liquid paraffin-infused porous surfaces, which achieved the surface wettability transition from liquid repellence to liquid adhesive [36]. Nevertheless, the adhesive between the substrate and coating of the LIS surfaces prepared by the aforementioned approaches needs to be enhanced to achieve improved serviceability. In addition, the surface transparency is also a crucial problem that cannot be overlooked in practical applications. It is arduous for most of the reported coatings to ensure an antireflective surface.

Here, we propose a versatile strategy for the design of slippery surfaces based on the construction of cross-linked polymer networks. A straightforward sol–gel procedure and spin-coating course were presented to prepare hydrophobic (HC) surfaces on a glass slide. Three kinds of silanes (TEOS, VTES and POTS) were polymerized into polymer networks after hydrolysis, which could firmly wrap the SiO_2 nanoparticles and form a pore-like structure for storing the infused lubricant for a long time. A commercial UV-curing adhesive was selected to reinforce the adhesive between the coating and matrixes. The prepared LIS surfaces with high mechanical robustness exhibited favorable repellency towards many types of liquids, as well as outstanding antireflective, anti-fouling, anti-icing and anti-corrosive properties. Furthermore, the synthesized sol and preparation process were also suitable for many kinds of substrates such as PET film, Al plate and Si plate.

2. Experiments

2.1. Materials

Tetraethylorthosilicat (TEOS, 98.0%) was obtained from Shantou XILONG Chemical Reagent Co. Inc., China, and vinyltriethoxysilane (VTES, 98.0%) was purchased from Sun Chemical Technology Co., Ltd, China. 1H,1H,2H,2H-perfluoroalkyltriethoxysilanes (POTS, >97.0%) were supplied by TCI, China. The DuPont Krytox perfluoroalkylpolyether (PFPE, >95.0%) GPL 103 lubricant was purchased from the Chemours Company. SiO_2 with a 20 nm diameter and a purity of 99.5% was purchased from Meryer Chemical Technology Co., Ltd. Moreover, the Glass slide, PET sheet, Si plate, Al plate and UV curing adhesive were commercially available. All other chemicals were of analytical-grade and were used as received. Deionized (DI) water was purified using a ModuPure system and used throughout the study.

2.2. Preparation of slippery surface

The fabrication procedure of LIS surfaces is schematically illustrated in Fig. 1. In the first step, precursor materials including TEOS, VTES, POTS, and SiO_2 were mixed in a beaker and magnetically stirred at 25 °C for 20 min. SiO_2 nanoparticles were used to bring forth the nanoscale roughness. In the second step, DI, normal propyl alcohol (NPA) and acetic acid were added into the precursor materials and stirred at 25 °C for 1 h to carry out the hydrolysis reaction of silanes. In this experiment, the molar ratio of the ingredients TEOS: VTES: POTS: H_2O: NPA: HAc was equal to 6 : 7 : 2 : 51 : 30 : 1, and the dosage of additional SiO_2 was 0.5 g. NPA served as a co-solvent to prepare the nanocomposite slurries. Next, the mixture was stirred for another 48 h under the same environmental conditions in order to produce nanosol. In the third step, the substrates were spin-coated with 0.5 ml of UV-curing adhesive using a vacuum spin coater (VTC-100, MTI Corporation). Then, another 1 ml of nanosol was spin-coated on the substrates. The obtained substrates coated with the nanosol and the UV curing adhesive were named hydrophobic (HC) surfaces. Further, the prepared HC surfaces were exposed to UV light for 5 min and then thermally treated at 65 °C for another 30 min. Afterwards, in order to obtain the LIS surfaces, 100 μl of PFPE was dropped onto HC surfaces using a pipette, and all samples were placed vertically for 3 min to remove the excess lubricant through gravity-driven drainage. The substrates included the glass slides, PET sheets, Si plates and Al plates.

2.3. Characterization

All photographs and videos were taken using a digital camera (Sony camera, DSCHX200). The images of the modified substrates' morphologies were taken using a field emission scanning electron microscope (FESEM, JSM-6701F) with Au-sputtered specimens. The three-dimensional surface imaging of the samples were identified

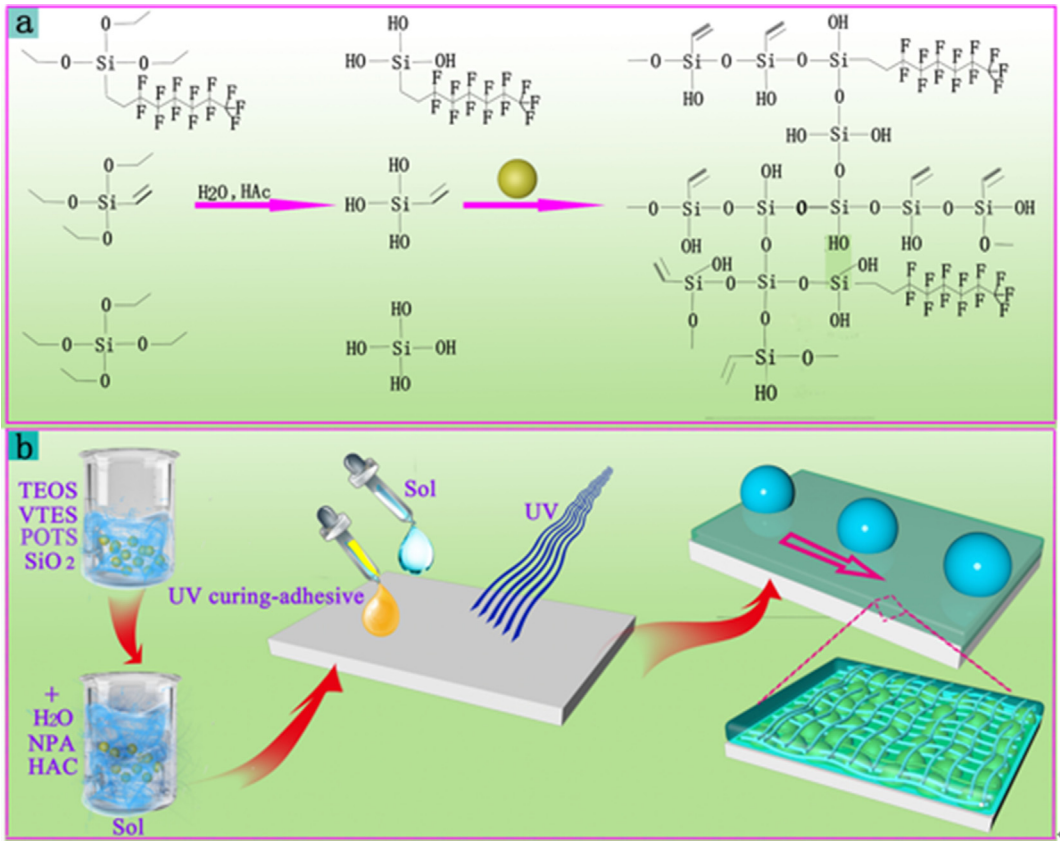

Fig. 1. (a) The hydrolysis and polymerization of silanes. (b) The schematic diagram of the preparation process of LIS surfaces.

using a surface imaging system atomic force microscopy (AFM, CSPM 5500). The chemical composition was analyzed via Fourier transform infrared spectroscopy (FTIR, Thermo Scientific Nicolet iS10), which was recorded as KBr disks on a Bruker 1600 FTIR spectrometer. The quantitative elemental composition was characterized by X-ray photoelectron spectroscopy (XPS, Thermo Scientific ESCALAB 250Xi). The contents of the chemical elements were analyzed by energy dispersive spectroscopy (EDS, JSM-5600LV). The water contact angles (WCAs) and oil contact angles (OCAs) were measured using a JC2000D system (Zhong chen Digital Equipment Co., Ltd., Shanghai, China) with distilled water and oil droplets (5 μl) at the ambient temperature. The sliding angles (SAs) were measured using a DSA100 contact angle meter. The average WCAs, OCAs and SAs were obtained by measuring the same sample at five different positions.

2.4. Stability tests

The stability tests of the modified surfaces were divided into two sections. (i) The mechanical stability of HC surfaces was measured by tape stripping, knife scratching, pencil scratching and sandpaper wiping (1000 mesh). (ii) The durability of LIS surfaces was measured by keeping the surfaces at 60 °C for one week. Subsequently, the sliding ability of water droplets on LIS surfaces at different times was measured. After all of these stability tests, the WCAs and SAs of these surfaces were measured.

2.5. Anti-fouling and self-cleaning property tests

The HC surfaces and LIS surfaces were immersed in milk, honey, coffee, and ketchup, and the cleanliness of these surfaces was observed after being immersed 1–60 times. Moreover, the ferromagnetic particles obtained by dispersing triiron tetroxide in ethylene glycol were used to remove the surface stains by means of introducing an external magnetic field to drive the particles.

3. Results and discussion

3.1. Fabrication and characterization of HC and LIS surfaces

The HC surfaces were prepared via the facile hydrolysis-polycondensation of silanes. Silanes have been extensively applied in building HC surfaces due to its hydrophobic property and the intrinsic rough structure of the substrates. In the present work, the surface fabrication process was illustrated in Fig. 1. As shown in Fig. 1a, three kinds of silanes (TEOS, VTES and POTS) were hydrolyzed and polymerized into the network structure under the induction of water and acetic acid [37,38]. There was a little SiO_2 produced by the hydrolysis of silanes. Hence, additional SiO_2 was added to create sufficient oil storage structures. Sol was formed through intertwining silane polymer with SiO_2 nanoparticles under magnetic agitation. After spin-coating, the smooth glass was covered by sol, thus forming a uniform and dense monolayer. Although there was a certain adhesion force between the matrix and nanosol, the coating was easily destroyed or shed when the surfaces were subjected to external friction, vibration and scratching by a hard object. To address this problem, herein, we put a transparent UV curing adhesive between the substrate and sol coating to firmly conglutinate the sol on the substrates (Fig. 1b). The UV curing adhesive could be solidified into a highly viscous, transparent adhesive layer under UV lamp irradiation [39]. The low surface roughness of the SiO_2 nanocoating and the substantial cross-linked networks gave rise to hydrophobicity instead of

superhydrophobicity in which the assembled nanoporous and network structures could firmly capture the PFPE lubricant [40].

To confirm the successful hydrolyzation and polymerization process, the chemical compositions of the sol were detected using FTIR and XPS. Moreover, the elemental distribution maps of the surfaces were analyzed using EDS. In the FTIR spectra (Fig. 2a), the vibration peak appearing at 1074 cm^{-1} was attributed to the stretching vibration of Si—O—Si, thereby corroborating that TEOS, VTES and POTS were polymerized together. The absorption peaks at 776 cm^{-1} and 461 cm^{-1} represented the stretching vibrations of Si—C and Si—O, respectively. The small absorption bands at 1604 cm^{-1} and 899 cm^{-1} represented the vinyl stretching vibration and the C—H bending vibration of vinyl, respectively. The absorption banks at 1413 cm^{-1} and 2920 cm^{-1} belonged to the stretching vibrations of C—F and methylene, respectively. The wide peak at 3431 cm^{-1} reflected the stretching vibration of the hydroxyl group. Furthermore, from the full survey spectrum of the XPS (Fig. 2b), the detected signals at 290, 105, 535 and 690 eV were ascribed to C1s, Si2p, O1 s and F1 s, respectively [41]. To further explore the distributions of these elements on the surface, EDS images were presented as shown in Fig. 2c, where the distributions of Si, O and C were significantly denser than F, and the content was also much higher than F. The reason for this phenomenon was that a very small amount of fluorosilane was used, and the matrix surfaces also contain Si, O and C elements.

For the matrix, we investigated the surface morphologies using a scanning electron microscope (SEM). Fig. 3a exhibited a typical SEM image of the nanocomposite polymer coating, which was randomly dotted with some protruding orifice-like structures. The surface appeared smooth at a low magnification, but a certain

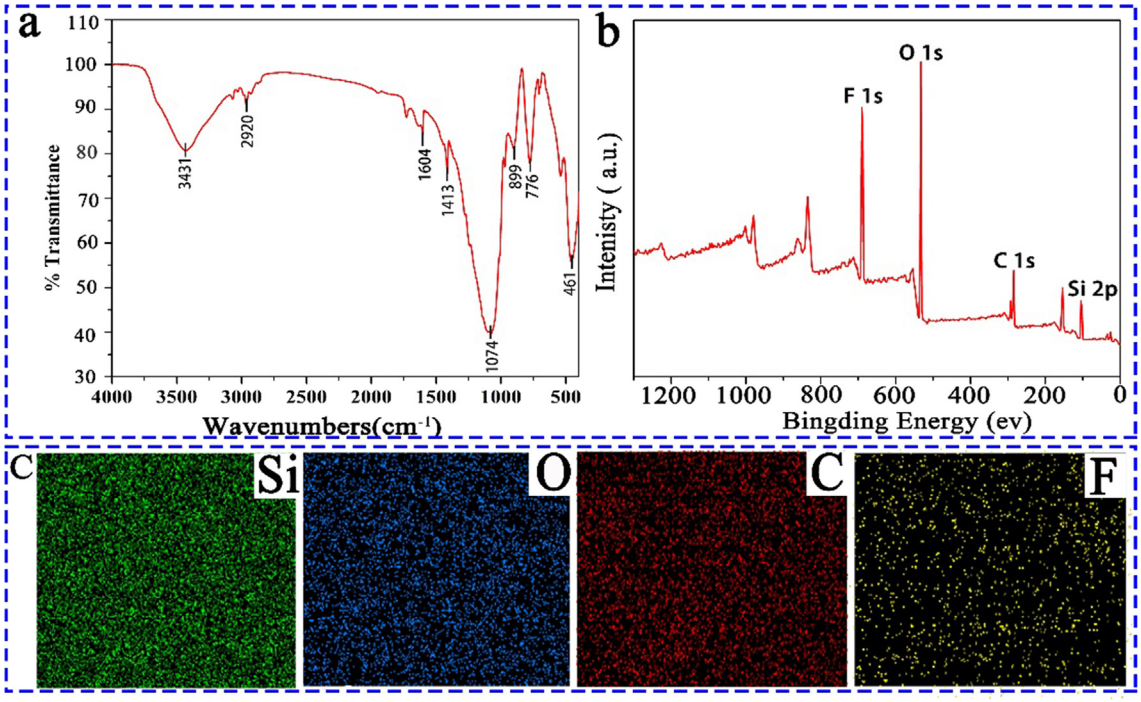

Fig. 2. Characterization of the prepared HC and LIS surfaces. (a) FTIR patterns of the synthetic sol. (b) XPS patterns of the synthetic sol. (c) EDS images of the Si, O, C and F distributions on HC surfaces.

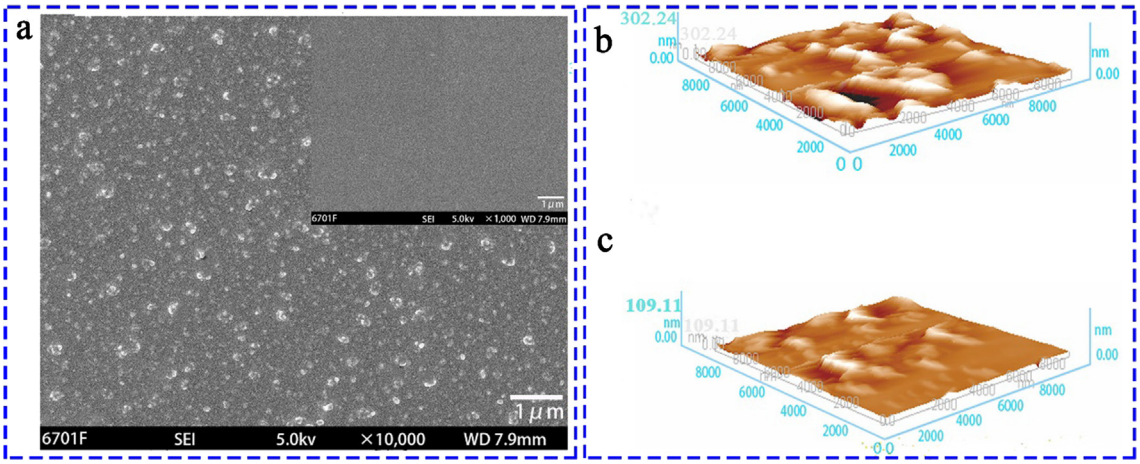

Fig. 3. (a) FESEM images of HC surfaces, and the inset panel was the low-magnification of the HC surfaces. (b) and (c) represented the AFM images of the HC and LIS surfaces, respectively.

roughness was revealed at a high magnification. These nanostructures were advantageous for achieving capillary action to facilitate the surface lubricant storage ability. In addition, we used the AFM to further explore the three-dimensional topography of the surface. The image displayed that nanosized protrudes were engendered on the HC surfaces, which produced a root-mean-square roughness (R_{rms}) of 41.2 nm (Fig. 3b). In contrast, the roughness of the LIS surfaces decreased significantly and the R_{rms} was only 18.3 nm (Fig. 3c) due to the formation of an oil film on the surfaces.

Compared with pure glass, the wettability of the HC and LIS surfaces were significantly reduced. The WCAs of pure glass and the HC and LIS surfaces were characterized as described in Fig. 4a–d. The WCAs of HC surfaces were 123 ± 1° (Fig. 4b) since the surfaces' roughness contributed to trapping air pockets in the cavities and prevented the surfaces from being wetted. In contrast, the WCAs decreased to approximately 112° after PFPE infusion (Fig. 4c). This can be attributed to the infused water-insoluble lubricant that occupied the cavities, thereby leaving no space for air. Thus, the assembled nanoporous structure firmly locked the PFPE and an obvious oil film formed between the droplet and substrate. In the experiment, a 5 μl droplet was used to detect the sliding-motion of the droplet on the surface. The results verified that the droplet could easily slide off the substrate when the surface was slightly tilted by 3°. The measured values of the advancing (θA) and receding (θR) WCAs were 112 ± 1° and 109 ± 1° (Fig. 4d, Movie S1 and Movie S2), respectively, thereby demonstrating that the droplet could slide easily on the surface because of the slight CA hysteresis of approximately 3°. To further explore the omniphobicity of the surface, another five organic compounds (glycol, dimethyl sulfoxide, methylbenzene, chlorobenzene and isooctane) were selected to detect the slip ability and wettability of different organic matters on the substrate (Figs. 4e and S1). The SAs for most of the tested liquids on the LIS surfaces were less than 5° apart from glycol, which had slightly larger SAs than other tested liquids, but it was still smaller than 10°. Hence, the results of all tests indicate that the LIS surfaces had excellent omniphobicity.

3.2. Antifouling and self-cleaning properties of LIS surfaces

Endowing artificial surfaces with antifouling and self-cleaning properties are of great significance for broadening the practical application of the materials [28]. To gain insight into the antifouling and self-cleaning ability of LIS surfaces, here, we investigated the wettability of four different kinds of everyday visible liquids on the surfaces. On the one hand, as shown in Fig. 5a, the original glass and LIS glass were vertically dipped into milk 60 times. To ensure that the slippery surfaces would not be contaminated by the dirty liquids, both sides of the glass were spin-coated with sol and infused with PFPE. The original glass was covered with milk as long as it was immersed into the bottle. Therefore, the original glass was always in a polluted state during the immersion from 1 dip to 60 dips. On the contrary, the LIS glass can maintain its original state throughout the impregnation process and remained uncontaminated by milk. In addition, we also tested the contamination of the two kinds of surfaces in high concentrations of honey, coffee and ketchup (Fig. 5b). The results illustrated that the LIS glass could lock the lubricant oil (PFPE) well and had outstanding antifouling ability.

On the other hand, a milk droplet (5 μl) could slip off the surface within 3 s when the slippery glass was tilted at approximately 4° (Fig. 5c). Moreover, in order to check whether the slippery surfaces could achieve the anti-fouling effect while horizontal, we first randomly sprinkled some graphite powder on the LIS glass. Then, a magnetic droplet (11 μl) was placed on the LIS surfaces and driven by an external magnetic field. The stains on the LIS glass could be wrapped in magnetic particles when the Fe_3O_4 particles freely moved back and forth on the surfaces. After the experiment, there was no trace of powder left on the surfaces and no visible graphite powder was observed to have penetrated into the slippery surface. We found that the graphite powder on the LIS surfaces could be cleaned up by the moving magnetic particle within 31 s (Fig. 6). Hence, we emphasized here that all experimental results showed that the LIS surfaces had superior anti-fouling and self-cleaning functions, whether they were vertical, inclined or horizontal. The proven merits of the slippery surfaces, such as its omniphobic, antifouling and self-cleaning properties, showed that the spin-coating approach for fabricating slippery surfaces was a proper choice. Further, the coating we prepared in this study also had a promising universality. Using the same spin-coated method, we prepared slippery surfaces on PET film, Si plate and Al plate, and found that the droplets could also fall freely on these surfaces in a short time (Fig. 7a–d). These useful properties of the coating showed that LIS surfaces could better adapt to practical applications, such as packaging, oil transport and so forth.

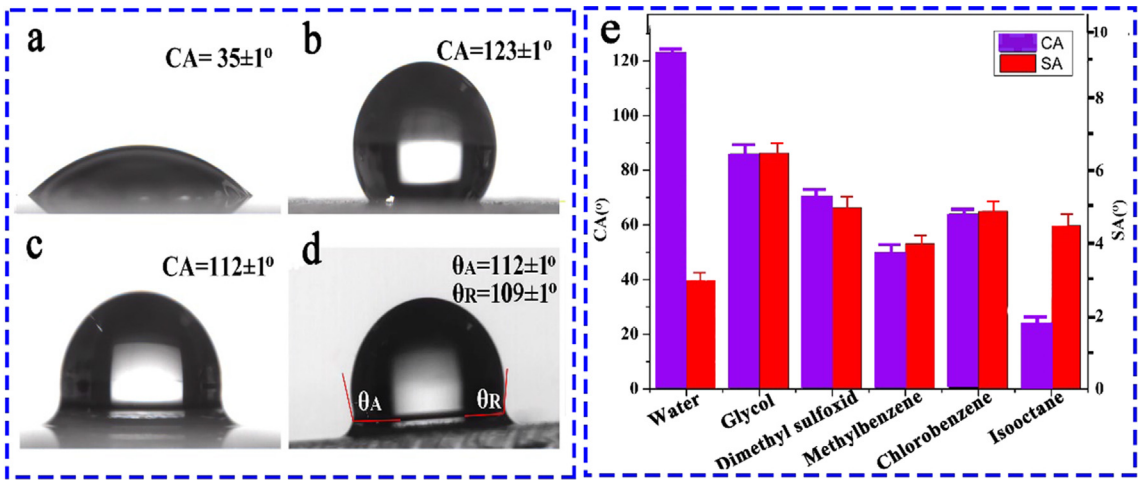

Fig. 4. Photographs of liquid droplets on glass. The static water droplet contact angle on (a) the original glass, (b) the textured hydrophobic glass and (c) the hydrophobic glass after PFPE infusion. (d) The dynamic motion of water droplets on the LIS surfaces, and (e) the contact angle (CA) and slide angle (SA) of various liquid droplets (water, glycol, dimethyl sulfoxid, methylbenzene, chlorobenzene and isooctane) on the LIS surfaces.

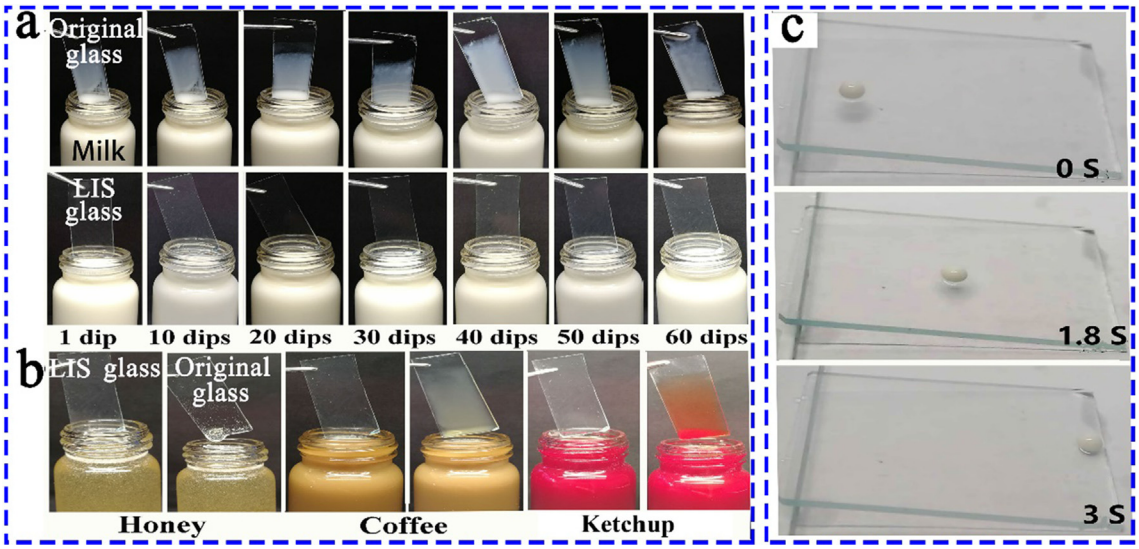

Fig. 5. A series of anti-fouling tests confirmed the self-cleaning performance of LIS glass when it was in a different placement state. (a) Vertically immersing the original and LIS glass in milk 1–60 times; (b) vertically immersing the original (right) and LIS (left) glass in honey, coffee and ketchup; and (c) milk droplet slip on tilted LIS glass.

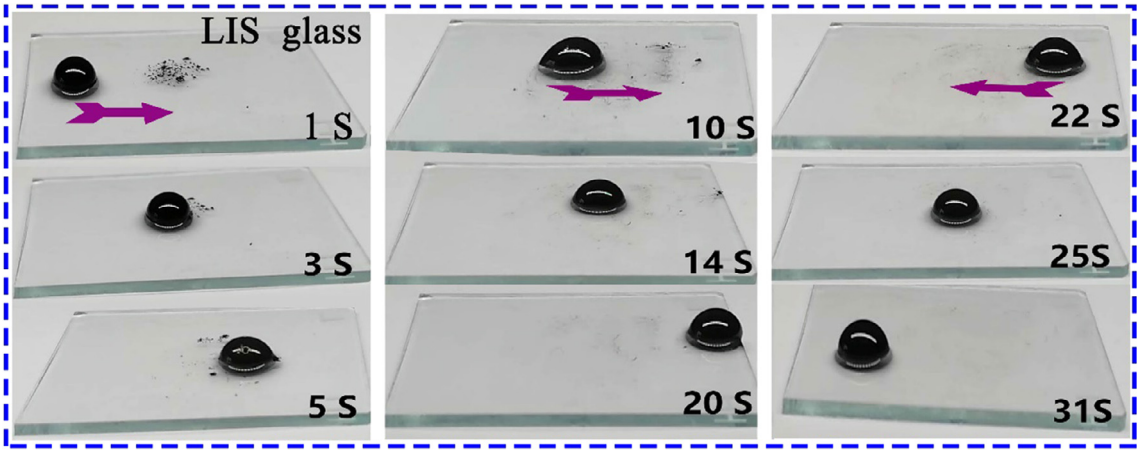

Fig. 6. The removal of stains on flatwise LIS glass using magnetic particles under the action of an applied magnetic field.

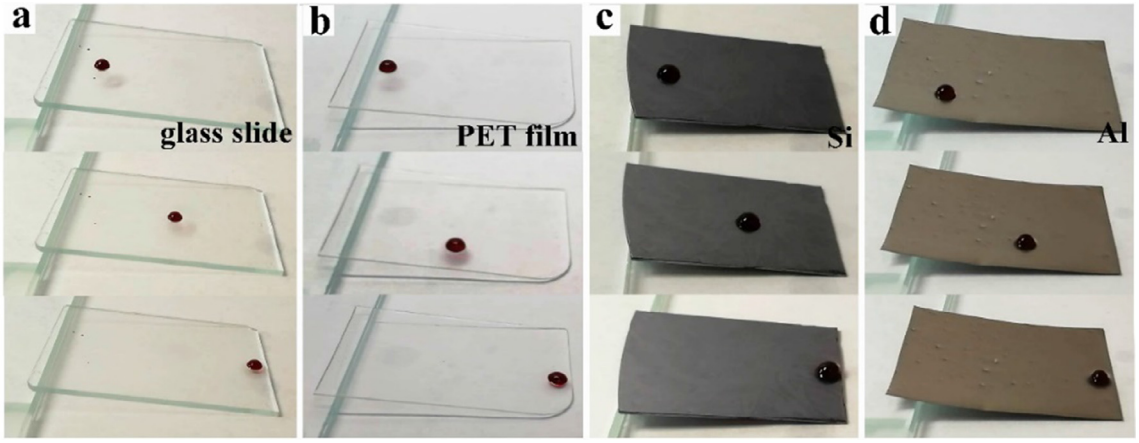

Fig. 7. Images showing ethylene glycol droplets (dyed with methyl red) sliding on (a) the glass slide, (b) the PET film, (c) the Si plate and (d) the Al plate.

3.3. Stability of LIS surfaces

Stability is an important index for evaluating the quality of materials, which will greatly affect the large-scale applications and further development of the prepared materials [42]. Therefore, it is necessary to do our best to improve the durability of new materials, which is also a vital problem many researchers have been trying to address. In the presented paper, we characterized the durability of LIS surfaces in terms of its mechanical strength and oil storage capacity. The mechanical property of the obtained LIS surfaces was measured using various means, such as tape stripping, sandpaper wiping (1000 mesh), knife scratching and pencil scratching (Fig. 8a). After various mechanical tests, the sliding abilities of water droplets on various damaged surfaces were detected. The results displayed that the SAs of water droplets on the LIS surfaces after 25 mechanical tests were not obviously different from the original undamaged surfaces. After various mechanical tests, the sliding angle of water droplets on the LIS surfaces increased slightly, but overall it was below 7°. Further, the contact angle of water droplets fluctuated approximately 112° (Fig. S2). Compared with the knife scratching and pencil scratching tests, the contact angle decreased slightly after the tape stripping and sandpaper wiping tests. This was mainly because tape stripping and sandpaper wiping had larger contact areas with the surfaces. Thus, the roughness and oil storage ability of the LIS surfaces were more likely to be affected. Overall, the contact angle and sliding angle did not change much. Moreover, after 25 mechanical tests, water droplets could still easily slide off the transparent LIS glass (Fig. S3). Hence, we concluded that the LIS surfaces we prepared had relatively stable mechanical resistance. From a theoretical perspective, this could be interpreted in two ways: (i) the anchoring strength of the solidified UV-curing adhesive firmly conglutinated the gel to the substrate and made it adhere better, and (ii) the surface structures made up of cross-linked polymer networks and SiO_2 were not easily destroyed. To further explore the stability of LIS surfaces, we measured the oil storage capacity of LIS surfaces by means of placing the LIS surfaces at 60 °C for one week. Then, the WCAs and SAs of the slippery surfaces were measured (Fig. 8b). The lubricant (PFPE) had promising stability and it would only volatilize a little, even at a high temperature. Therefore, the contact angle and sliding angle of water droplets increased with the volatilization of the lubricant, but it changed only slightly. Overall, it was suggested that the surface had a relatively stable slippery performance during the testing.

3.4. Optical, anti-corrosion and anti-icing properties

To explore the multi-functionality of the prepared surfaces, here, the anti-icing, optical and anti-corrosion properties were addressed. Ice accumulation on solid surfaces has a great effect on aircrafts, power lines, vessels and so forth, leading to irretrievable losses and catastrophies [43]. The anti-icing and ice-phobic properties were indispensable for most functional surfaces when it was required for a wider range of practical applications. As shown in Fig. 9, the prepared LIS glass confirmed its anti-icing ability on account of the lack of pinning spots for water molecular aggregation and nucleation, which could effectively postpone the formation of critical ice nuclei and decrease the growth rate of ice crystals. To observe the anti-icing process, water droplets with a volume of 8 μl were placed on the super-cooled HC and LIS glass at −10 ± 1 °C (Fig. 9a). The droplet on the HC glass was clear and transparent at the beginning. Afterwards, white ice crystals appeared in the droplet at 302 s, and some frost appeared on the surface at 403 s. Finally, at 605 s, the droplet turned completely into an opaque ice droplet and adhered to the surface. It indicated that the HC glass could postpone water freezing, but the delay time (DT) was not long enough. In contrast, the droplet on the LIS glass remained a transparent liquid that did not freeze until 1220 s,

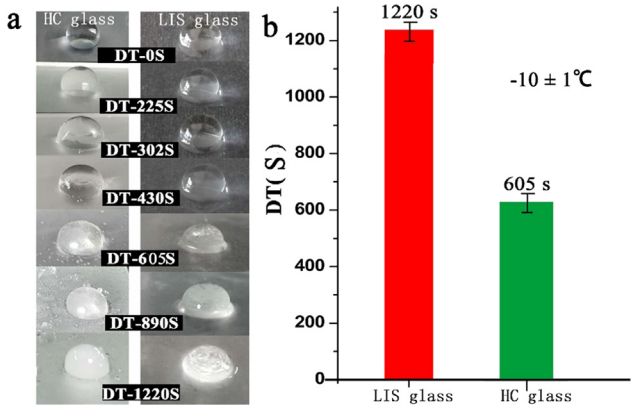

Fig. 9. (a) Ice accumulation on the HC and LIS glass at −10 ± 1 °C with the delay times (DT) roughly recorded by observing the non-transparency of the water droplets. (b) The LIS glass had a much longer DT of 1220 s than the HC glass with a DT of 605 s.

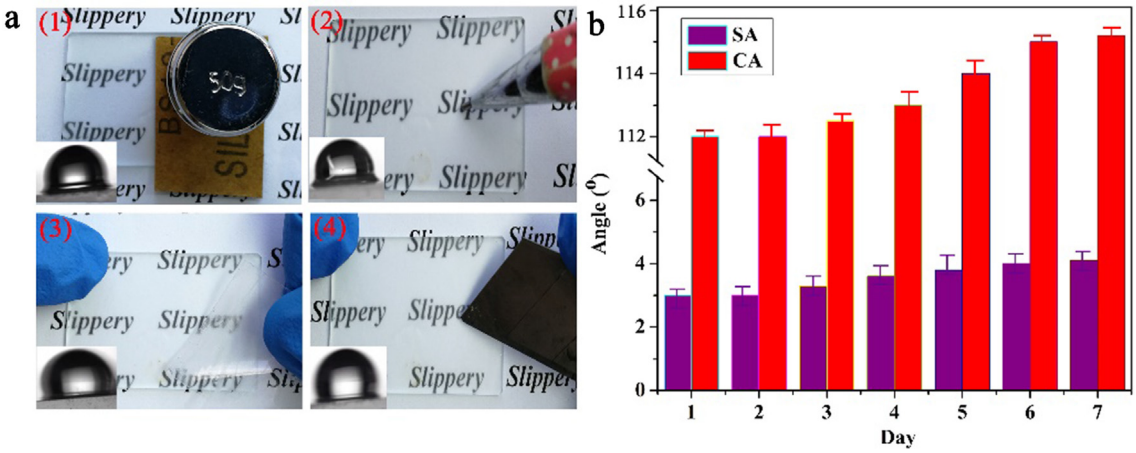

Fig. 8. (a) Mechanical stability tests of HC glass: (1) sandpaper wiping, (2) pencil scratching, (3) tape stripping, and (4) knife scratching. The embedded images show the sliding behaviors of water droplets on each slippery surface after 25 tests. (b) The WCAs and SAs of the water droplet measured on LIS surfaces, which are placed at 60 °C for 1–7 days.

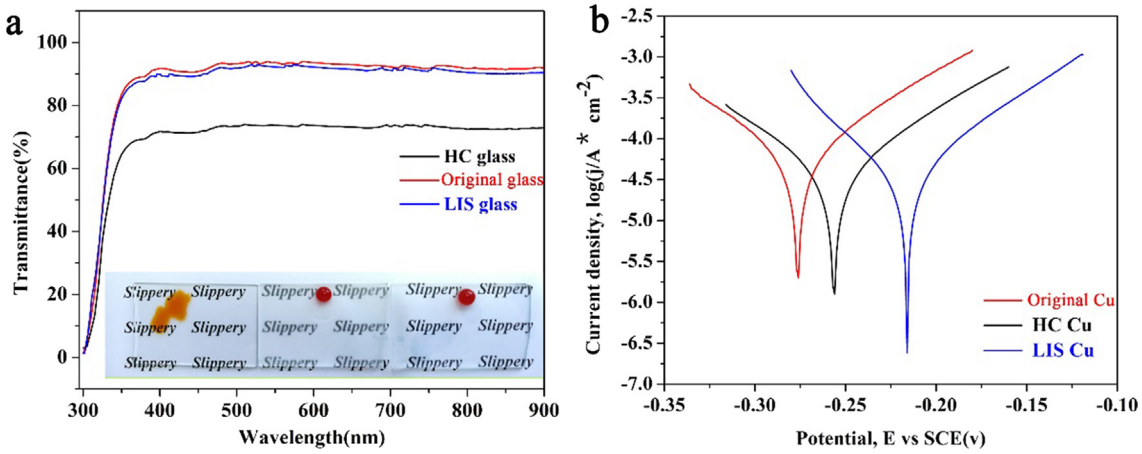

Fig. 10. (a) Optical transmittance spectra and photographs (inset) of the original (left), HC (middle) and LIS (right) glass. (b) The electrochemical corrosion tests of the prepared HC and LIS for Cu and the original Cu in a 3.5 wt% NaCl solution.

thereby demonstrating that the LIS glass possessed a better ability to restrain ice formation and accumulation (Fig. 9b). There were main two reasons for the difference between the two surface delay icing times (DT). (i) For HC surfaces, the high roughness would lead to a large contact area between the droplet and surface. Consequently, ice crystals were easily formed on these contact areas. This was the main reason why the HC surfaces' freeze delay time (DT) was short. (ii) As a result of the capillary and gravity effects, the lubricant oil could permeate into the roughness of the surface and form a homogeneous and smooth oil film on the surface. After lubricant (PFPE) infusion, the smooth oil film could both isolate the direct contact between the droplet and surface, and also reduce the nucleation probability of the droplet and the water/ice adhesion force. Hence, compared to HC surfaces, LIS surfaces had a longer freeze delay time. Actually, all of presented multi-functional surfaces can only delay ice accumulation rather than completely eliminate ice formation. Hence, the fabrication of ice-phobic surfaces remains a challenging problem.

Generally, the optical property is indispensable for something made of glass. The optical transmittance spectra of the original, HS and LIS glass are shown in Fig. 10a. Compared with the HC glass, the LIS glass had superior transparency in the visible wavelength range. The visible-light transparency of the original glass was approximately 92%, whereas the HC glass was nearly in a semi-transparent state and the transparency was approximately 70% on account of the diffuse reflectance of light by the rough structure. After being infused with lubricant, the transparency of the LIS glass was almost that of the original surface (inset photos of Fig. 10a). This was mainly because the LIS glass was intensely thin and smooth enough, and the glossy lubricant film could prevent the reflection of visible light. Furthermore, the transmittance of light would not be affected by the UV-curing adhesive because it was smooth and transparent after curing. Hence, this kind of surface preparation procedure and coating can be used to fabricate stable slippery surfaces with an excellent antireflective property. This kind of transparent slippery surface can be applied in solar cells. The outstanding self-cleaning ability is able to enhance the collection efficiency of sunlight, and the anti-icing performance can improve surface adaptability to harsh environments [44–46].

To further explore other functions of LIS surfaces, slippery copper plates were obtained by using the same spin-coating method to detect whether the coating could endow the metallic substrate with anti-corrosion performance. Here, the potentiodynamic polarization curves for the hydrophobic copper plate, the slippery copper plate and original copper plate in a 3.5 wt% NaCl solution were carried out via electrochemical corrosion tests (Fig. 10b). In the typical polarization curves, the higher corrosion potential (E_{corr}) and lower corrosion current density (I_{corr}) of the tested materials signified a better anti-corrosion ability [47]. The E_{corr}s of the original copper plate, the HC copper plate and the LIS copper plate were −0.279 eV, −0.258 eV, and −0.213 eV, respectively. The correctly computed I_{corr}s of the original copper plate, the HC copper plate and the LIS plate were 7.354×10^{-5} Acm^{-2}, 6.102×10^{-5} Acm^{-2}, and 3.378×10^{-5} Acm^{-2}, respectively. This means that the original Cu plate had the highest negative potential and the highest positive current. Further, the results indicated that spin-coated surfaces possessed preferable corrosion resistance when compared to original copper. This phenomenon was able to be interpreted by the existence of an air layer on HC copper, which prevented direct contact between the solution and the surface such that the electrolytic reaction was largely suppressed. The lubricant film on the slippery copper could further insulate the solution and the surface. Consequently, the electrolytic reaction was further inhibited such that the LIS Cu plate had a better anti-corrosion property than that of the HC Cu plate. From all the above statements, we concluded that the LIS surfaces fabricated by the spin procedure had excellent anti-icing, optical and anti-corrosion performance, which provided inspiration for the preparation of multi-functional slippery surfaces.

4. Conclusions

To summarize, lubricant-infused slippery surfaces have been reported on in previous publications [9,50]. However, the transparency of slippery materials and the adhesion between the coating and substrate still need to be improved. Taking inspiration from some previously reported strategies [48,49], here a kind of coating related to the hydrolysis and polymerization of three kinds of silanes (TEOS, VTES and POTS) has been reported. A slippery lubricant (PFPE) infused surface has been prepared via the combination of SiO_2 nanoparticles and the network structure generated from these silanes. Unlike other works that suggested directly spin-coating the nanosol on the substrates [37,40], we spin-coated an extra UV-curing adhesive between the substrate and sol. Subsequently, the use of a transparent UV curing adhesive can bind the coating firmly to the substrate and improve the mechanical stability of the LIS surfaces without affecting the transparency of the surfaces. In addition, the lubricant-infused surfaces can repel various liquids and exhibit a multitude of excellent

properties, such as antifouling, self-cleaning, liquid-repellence, anti-icing, and anti-corrosion. More importantly, the PFPE infused surfaces possessed a profound antireflective ability and mechanical robustness even after several stability tests, and these are properties that are conducive to preparing durable and transparent slippery surfaces. We believe that this coating and its preparation method can be helpful for the design and manufacture of progressive and multifunctional interface materials. The prepared LIS surfaces also provide practical applications for the fields of liquid transportation, antifouling, solar cells, etc.

Acknowledgement

This work is supported by the National Nature Science Foundation of China (No. 51522510, 51675513, and 51735013).

Appendix A. Supplementary material

Supplementary data to this article can be found online at https://doi.org/10.1016/j.jcis.2018.10.083.

References

[1] M.Y. Cao, X. Jin, Y. Peng, C.M. Yu, K. Li, K.S. Liu, L. Jiang, Unidirectional wetting properties on multi bioinspired magnetocontrollable slippery microcilia, Adv. Mater. 29 (2017) 1606869.
[2] Y. Cui, D. Li, H. Bai, Bioinspired smart materials for directional liquid transport, Ind. Eng. Chem. Res. 56 (2017) 4887.
[3] S. Deng, W. Shang, S. Feng, S. Zhu, Y. Xing, D. Li, Y. Hou, Y. Zheng, Controlled droplet transport to target on a high adhesion surface with multi-gradients, Sci. Rep. 7 (2017) 45687.
[4] X.C. Chen, K.F. Ren, J. Wang, W.X. Lei, J. Ji, Infusing lubricant onto erasable microstructured surfaces toward guided sliding of liquid droplets, ACS Appl. Mater. Interfaces 9 (2017) 1959.
[5] J.A. Lv, Y.Y. Liu, J. Wei, E. Chen, L. Qin, Y.L. Yu, Photocontrol of fluid slugs in liquid crystal polymer microactuators, Nature 537 (2016) 179–184.
[6] T. Zhou, J. Yang, D. Zhu, J. Zheng, S. Handschuh-Wang, X. Zhou, J. Zhang, Y. Liu, Z. Liu, C. He, X. Zhou, Hydrophilic sponges for leaf-inspired continuous pumping of liquids, Adv. Sci. 4 (2017) 1700028.
[7] L. Ionov, N. Houbenov, A. Sidorenko, M. Stamm, S. Minko, Smart microfluidic channels, Adv. Funct. Mater. 16 (2006) 1153–1160.
[8] K. Manabe, K.H. Kyung, S. Shiratori, Biocompatible slippery fluid-infused films composed of chitosan and alginate via layer-by-layer self-assembly and their antithrombogenicity, ACS Appl. Mater. Interfaces 7 (2015) 4763–4771.
[9] A. Venault, H. Yang, Y. Chiang, B. Lee, R. Ruaan, Y. Chang, Bacterial resistance control on mineral surfaces of hydroxyapatite and human teeth via surface charge-driven antifouling coatings, ACS Appl. Mater. Interfaces 6 (2014) 3201–3210.
[10] J. Chen, K.Y. Li, S.W. Wu, J. Liu, K. Liu, Q.R. Fan, Durable anti-icing coatings based on self-sustainable lubricating layer, ACS Omega 2 (2017) 2047–2054.
[11] P. Kim, T.S. Wong, J. Alvarenga, M.J. Kreder, W.E. Adorno-Martinez, J. Aizenberg, Liquid-infused nanostructured surfaces with extreme anti-ice and anti-frost performance, ACS Nano 6 (2012) 6569–6577.
[12] J. Chen, R. Dou, D.P. Cui, Q.L. Zhan, Y.F. Zhang, F.J. Xu, X. Zhou, J.J. Wang, Y.L. Song, L. Jiang, Robust prototypical anti-icing coatings with a self-lubricating liquid water layer between ice and substrate, ACS Appl. Mater. Interfaces 5 (2013) 4026–4030.
[13] L. Feng, S. Li, Y. Li, H. Li, L. Zhang, J. Zhai, Y. Song, B. Liu, L. Jiang, D. Zhu, Superhydrophobic surfaces: from natural to artificial, Adv. Mater. 14 (2002) 1857.
[14] Y. Zheng, X. Gao, L. Jiang, Directional adhesion of superhydrophobic butterfly wings, Soft Matter. 3 (2007) 178–182.
[15] Y. Zheng, H. Bai, Z. Huang, X. Tian, F.Q. Nie, Y. Zhao, J. Zhai, L. Jiang, Directional water collection on wetted spider silk, Nature 463 (2010) 640.
[16] Z.Z. Gu, H. Uetsuka, K. Takahashi, R. Nakajima, H. Onishi, A. Fujishima, O. Sato, Structural color and the lotus effect, Angew. Chem., Int. Ed. 42 (2003) 894–897.
[17] M. Liu, Y. Hou, J. Li, L. Tie, Y. Peng, Z. Guo, Inorganic adhesives for robust, self-healing, superhydrophobic surfaces, J. Mater. Chem. A. 5 (2017) 19297–19305.
[18] Y. Hu, Y. Zhu, H. Wang, C. Wang, H. Li, X. Zhang, R. Yuan, Y. Zhao, Facile preparation of superhydrophobic metal foam for durable and high efficient continuous oil-water separation, Chem. Eng. J. 322 (2017) 157–166.
[19] S. Farhadi, M. Farzaneh, S.A. Kulinich, Anti-icing performance of superhydrophobic surfaces, Appl. Surf. Sci. 257 (2011) 6264–6269.
[20] N.W.L.L. Tang, W. Tong, D.S. Xiong, Fabrication of robust and scalable superhydrophobic surfaces and investigation of their anti-icing properties, Mater. Des. 156 (2018) 320–328.
[21] T.K. Chen, Q. Cong, Y.C. Qi, J.F. Jin, K.L. Choy, Hydrophobic durability characteristics of butterfly wing surface after freezing cycles towards the design of nature inspired anti-icing surfaces, PloS One 13 (2018). e0188775.
[22] S.S. Jia, H.B. Chen, S. Luo, Y. Qing, S.L. Deng, N. Yan, Y.Q. Wu, One-step approach to prepare superhydrophobic wood with enhanced mechanical and chemical durability: Driving of alkali, Appl. Surf. Sci. 455 (2018) 115–122.
[23] X. Zhang, D.F. Zhi, L. Sun, Y.B. Zhao, M.K. Tiwari, C.J. Carmalt, L.P. Parkin, Y. Lu, Super-durable, non-fluorinated superhydrophobic free-standing items, J. Mater. Chem. A 6 (2018) 357–362.
[24] J.A. Moran, C.M. Clarke, The carnivorous syndrome in Nepenthes pitcher plants: current state of knowledge and potential future directions, Plant Signaling Behav. 5 (2010) 644–648.
[25] T.S. Wong, S.H. Kang, S.K.Y. Tang, E.J. Smythe, B.D. Hatton, A. Grinthal, J. Aizenberg, Bioinspired self-repairing slippery surfaces with pressure-stable omniphobicity, Nature 477 (2011) 443–447.
[26] K.C. Park, P. Kim, A. Grinthal, N. He, D. Fox, J.C. Weaver, J. Aizenberg, Condensation on slippery asymmetric bumps, Nature 531 (2016) 78–82.
[27] H. Chen, P. Zhang, L. Zhang, H. Liu, Y. Jiang, D. Zhang, Z. Han, L. Jiang, Continuous directional water transport on the peristome surface of Nepenthes alata, Nature 532 (2016) 85–89.
[28] X. Hou, Y. Hu, A. Grinthal, M. Khan, J. Aizenberg, Liquid-based gating mechanism with tunable multiphase selectivity and antifouling behaviour, Nature 519 (2015) 70–73.
[29] J. Li, L. Li, X. Du, W. Feng, A. Welle, O. Trapp, M. Grunze, M. Hirtz, P.A. Levkin, Reactive superhydrophobic surface and its photoinduced disulfide-ene and thiol-ene (bio) functionalization, Nano Lett. 15 (2015) 675–681.
[30] Y. Huang, B.B. Stogin, N. Sun, J. Wang, S.K. Yang, T.S. Wong, A switchable cross-species liquid repellent surface, Adv. Mater. 29 (2017) 1604641.
[31] Y. Wang, H.F. Zhang, X.W. Liu, Z.P. Zhou, Slippery liquid-infused substrates: a versatile preparation, unique anti-wetting and dragreduction effect on water, J. Mater. Chem. A 4 (2016) 2524–2529.
[32] P. Wang, D. Zhang, S.M. Sun, T.P. Li, Y. Sun, Fabrication of slippery lubricant-infused porous surface with high underwater transparency for the control of marine biofouling, ACS Appl. Mater. Interfaces 9 (2017) 972–982.
[33] U. Manna, D.M. Lynn, Fabrication of liquid-infused surfaces using reactive polymer multilayers: principles for manipulating the behaviors and mobilities of aqueous fluids on slippery liquid interfaces, Adv. Mater. 27 (2015) 3007–3012.
[34] U. Manna, N. Raman, M.A. Welsh, Y.M. Zayas-Gonzale, H.E. Blackwell, S.P. Palecek, D.M. Lynn, Slippery liquid-infused porous surfaces that prevent microbial surface fouling and kill non-adherent pathogens in surrounding media: a controlled release approach, Adv. Funct. Mater. 26 (2016) 3599–3611.
[35] M.J. Coady, M. Wood, G.Q. Wallace, K.E. Nielsen, A.M. Kietzig, F.L. Labarthet, P.J. Ragogna, Icephobic behavior of UV-cured polymer networks incorporated into slippery lubricant-infused porous surfaces: improving SLIPS durability, ACS Appl. Mater. Interfaces 10 (2018) 2890–2896.
[36] K. Manabe, T. Matsubayashi, M. Tenjimbayashi, T. Moriya, Y. Tsuge, K.H. Kyung, S. Shiratori, Controllable broadband optical transparency and wettability switching of temperature activated solid/liquid-infused nanofibrous membranes, ACS Nano 10 (2016) 9387–9396.
[37] C.Q. Wei, G.F. Zhang, Q.H. Zhang, X.L. Zhan, F.Q. Chen, Silicone oil-infused slippery surfaces based on sol−gel process- induced nanocomposite coatings: a facile approach to highly stable bioinspired surface for biofouling resistance, ACS Appl. Mater. Interfaces 8 (2016) 34810–34819.
[38] Y. Tang, Q. Zhang, X. Zhan, F. Chen, Superhydrophobic and anti-icing properties at overcooled temperature of a fluorinated hybrid surface prepared via a sol-gel process, Soft Matter. 11 (2015) 4540–4550.
[39] F. Chen, J. Song, Y. Lu, S. Huang, X. Liu, J. Sun, C.J. Carmalt, I.P. Parkin, W. Xu, Creating robust superamphiphobic coatings for both hard and soft materials, J. Mater. Chem. A 3 (2015) 20999–21008.
[40] M.M. Liu, Y.Y. Hou, J.L. Li, Z.G. Guo Tie, Transparent slippery liquid-infused nanoparticulate coatings, Chem. Eng. J. 337 (2018) 462–470.
[41] T. Rangel, A. Michels, F. Horowitz, D. Weibel, Superomniphobic and easily repairable coatings on copper substrates based on simple immersion or spray processes, Langmuir 31 (2015) 3465–3472.
[42] K. Golovin, M. Boban, J.M. Mabry, A. Tuteja, Designing self-healing superhydrophobic surfaces with exceptional mechanical durability, ACS Appl. Mater. Interfaces 9 (2017) 11212–11223.
[43] Q. Li, Z.G. Guo, Fundamentals of icing and common strategies for designing biomimetic anti-icing surfaces, J. Mater. Chem. A 6 (2018) 13549–13581.
[44] Y.B. Park, H. Im, M. Im, Y.K. Choi, Self-cleaning effect of highly water-repellent microshell structures for solar cell applications, J. Mater. Chem. 21 (2011) 633–636.
[45] X. Deng, L. Mammen, Y. Zhao, P. Lellig, K. Müllen, C. Li, H.J. Butt, D. Vollmer, Transparent, thermally stable and mechanically robust superhydrophobic surfaces made from porous silicia capsules, Adv. Mater. 23 (2011) 2962–2965.
[46] L.Q. Chen, A. Geissler, E. Bonaccurso, K. Zhang, Transparent slippery surfaces made with sustainable porous cellulose lauroyl ester films, ACS Appl. Mater. Interfaces 6 (2014) 6969–6976.
[47] W. Xu, J. Song, J. Sun, Y. Lu, Z. Yu, Rapid fabrication of large-area, corrosion-resistant super-hydrophobic Mgalloy surfaces, ACS Appl. Mater. Interf. 3 (2011) 4404–4414.
[48] L.M. Wang, T.J. McCarthy, Covalently attached liquids: instant omniphobic surfaces with unprecedented repellency, Angew. Chem. 128 (2016) 252–256.
[49] X. Yao, S.W. Wu, L. Chen, J. Ju, Z.D. Gu, M.J. Liu, J.J. Wang, L. Jiang, Self-replenishable anti-waxing organogel materials, Angew. Chem. 127 (2015) 9103–9107.
[50] P.S. Brown, B. Bhushan, Liquid-impregnated porous polypropylene surfaces for liquid repellency, J. Colloid Interface Sci. 487 (2017) 437–443.